

## Energy-loss effects in multiple-scattering angular distributions of ions in matter

Jorge E. Valdés

*Departamento de Física, Universidad de Santiago de Chile, C.C. 307, Santiago, Chile*

Néstor R. Arista

*División Colisiones Atómicas, Instituto Balseiro and Centro Atómico Bariloche, 8400 Bariloche, Argentina*

(Received 19 April 1993)

The standard theory of multiple scattering of ions traversing matter assumes that the energy loss of a particle, during transit through a medium, is very small compared with its initial energy. Here we consider the effect of finite-energy losses on the multiple-scattering angular distributions, by taking into account the variation of the energy-dependent scattering cross section as a function of the depth penetrated into the material. The theory is generalized to account for a continuous slowing down of the beam particles. We study in particular, for the case of slow ions, the increased spread of the angular distributions due to the energy-loss effect.

PACS number(s): 34.50.Bw, 61.80.Jh

### I. INTRODUCTION

The multiple scattering of swift ions traversing both gaseous and condensed media is one of the basic processes of interest for studies on the interaction of ion beams with matter. The basic theory of this phenomenon was developed many years ago by Goudsmit and Saunderson [1], Molière [2], and Snyder and Scott [3]. A complete review of the earlier developments was given by Scott [4].

One of the main effects of the multiple scattering is the observed angular spread of an initially well-collimated ion beam after passing through a medium [5–9]. The studies of this process provide an experimental test of the theoretical models on the multiple scattering of swift ions in solids. In particular, the calculations based in the small-angle approximation [10,11] permit us to obtain useful scaling laws in terms of reduced variables; the tabulations of the multiple-scattering function are widely used in ion-penetration studies and applications. A good agreement with experiments has been reported, both for gaseous and amorphous solid targets [5–8, 12].

One of the simplifying assumptions usually made in the treatment of the multiple-scattering process is to neglect the energy loss of the ions during transit through the target. Although in many experiments this assumption is satisfied, it is necessary to have a better knowledge of the corrections that arise if the energy loss of the particles is not negligible, as for instance in ion-beam transmission through thick targets or in ion implantation studies. The energy-loss effect in the multiple scattering of ions was recently discussed by Sigmund [9].

In particular, in recent experiments using thick polyester targets the influence of energy loss on the multiple-scattering angular distributions has been determined [13]. The increased values of the angular spreads with respect to the theoretical predictions have been explained by taking into account the lower values of the average energy of the ions, due to their slowing down in the foil.

The purpose of this paper is to consider the effect of the energy loss on the multiple-scattering process, and to

evaluate the spread of the angular distributions. The paper is organized as follows: in Sec. II the basic multiple-scattering equations are summarized; the energy-loss effect is introduced in Sec. III, and Sec. IV contains the results of calculations using the cross sections derived from the universal-potential model. An application to the case of slow ions in solids is considered. Section V summarizes the conclusions of this work.

### II. BASIC MULTIPLE-SCATTERING EQUATIONS

Following the usual notation [11,14], the differential scattering cross section  $d\sigma$ , for incident ions with mass  $M_1$  and atomic number  $Z_1$ , in a target characterized by the atomic number  $Z_2$  and mass  $M_2$ , can be cast in the form

$$d\sigma = \frac{\pi a^2}{2} t^{-3/2} f(t^{1/2}) dt, \quad (1)$$

where  $t$  is the reduced energy-angle variable, usually written as

$$t^{1/2} = \varepsilon \sin(\vartheta/2), \quad (2)$$

in terms of the center-of-mass scattering angle  $\vartheta$ , and reduced energy

$$\varepsilon = \frac{EaM_2}{Z_1 Z_2 e^2 (M_1 + M_2)}. \quad (3)$$

Here  $E$  is the ion energy in the laboratory system, and  $a$  is the screening parameter.

The scattering function  $f(t^{1/2})$  in Eq. (1) can be determined (e.g., by numerical integration) from the appropriate interatomic potential [14].

In the small-angle approximation, the angular distribution of ions,  $F(x, \alpha)$ , after traversing a foil of thickness  $x$ , can be written as [10,11]

$$F(x, \alpha) d\Omega = \frac{d\Omega}{2\pi} \int_0^\infty dk k J_0(k\alpha) e^{-Nx\sigma_0(k)}, \quad (4)$$

with

$$\sigma_0(k) = \int_0^\infty d\sigma [1 - J_0(k\phi)] . \quad (5)$$

Here  $\alpha$  is the total deflection angle,  $d\Omega$  is the solid-angle element around  $\alpha$ ,  $\phi$  is the single-collision laboratory scattering angle, and  $J_0(x)$  denotes the zero-order Bessel function.

To make use of the scaling properties of the scattering equations, it is convenient to introduce the reduced thickness  $\tau$  and the reduced angle  $\bar{\alpha}$ , defined by

$$\tau = \pi a^2 N x , \quad (6a)$$

$$\bar{\alpha} = \beta \alpha , \quad (6b)$$

where  $N$  is the number of target atoms per unit volume, and  $\beta$  represents the ion energy in appropriate units, viz.,

$$\beta = \frac{Ea}{2Z_1 Z_2 e^2} . \quad (7)$$

Then, Eq. (4) can cast in the simple form

$$F(x, \alpha) d\Omega = \bar{\alpha} d\bar{\alpha} f_1(\tau, \bar{\alpha}) . \quad (8)$$

The function  $f_1(\tau, \bar{\alpha})$  is a universal multiple-scattering function given by [10,11]

$$f_1(\tau, \bar{\alpha}) = \int_0^\infty dz z J_0(\bar{\alpha} z) e^{-\tau \Delta(z)} . \quad (9)$$

The relation between the integration variables in Eqs. (4) and (9) is  $z = k/\beta$ , while the scattering function  $\Delta(z)$  in Eq. (9) can be calculated from

$$\Delta(z) = \int_0^\infty d\bar{\phi} f(\bar{\phi}) / (\bar{\phi}^2) [1 - J_0(z\bar{\phi})] , \quad (10)$$

by integrating over the reduced laboratory scattering angle  $\bar{\phi}$ , defined by

$$\bar{\phi} = \beta \phi . \quad (11)$$

The important scaling parameter in this formulation is the reduced energy  $\beta$  (here a constant value) of Eq. (7).

### III. INCLUSION OF ENERGY-LOSS EFFECTS

The standard multiple-scattering theory, as summarized in the preceding section, is based on the assumption that the energy loss of the ions during their transit through the target is very small with respect to the initial energy. In cases where this condition is not satisfied one must take into account the variation of the differential scattering cross section  $d\sigma$ , and of the function  $\sigma_0(k)$  in Eqs. (4) and (5), with ion energy  $E$ . If the ion energy loss is described as a continuous process, one should integrate the effects over a range of ion energies  $E_0 < E < E_1$ . In the following,  $E_0$  and  $E_1$  will denote the mean energies of the incident and transmitted ion-beam particles.

For random media, each single-scattering process can be considered independent of the previous scattering events, as well as from the accumulated effects of the multiple scattering. Then, the continuous variation of the ion energy  $E(x')$  with penetration depth  $x'$  can be included in the calculation of the multiple-scattering distribution, Eq. (4), by the simple substitution [11]

$$\begin{aligned} \exp[-Nx\sigma_0(k)] &\Rightarrow \exp[-\Sigma(k, x)] \\ &\equiv \exp\left[-N \int_0^x dx' \sigma_0(k, E(x'))\right] , \end{aligned} \quad (12)$$

where the variation of the scattering cross section with the instantaneous ion energy  $E(x')$  is shown explicitly.

The function  $\sigma_0(k, E(x'))$  is calculated from Eqs. (1) and (5), with a variable energy  $E(x')$ . This yields

$$\sigma_0(k, E(x')) = \pi a^2 \Delta(z') , \quad (13)$$

and, therefore, Eq. (12) can be cast in the form

$$\exp[-\Sigma] = \exp\left[-\int_0^\tau d\tau' \Delta(z')\right] , \quad (14)$$

with

$$\Delta(z') = \int_0^\infty \frac{ds}{s^2} f(s) [1 - J_0(z's)] , \quad (15)$$

$$z' = \frac{k}{\beta(\tau')} , \quad (16)$$

and

$$\beta(\tau') = \frac{E(x')}{(2Z_1 Z_2 e^2/a)} . \quad (17)$$

In order to calculate the value of  $\Sigma$  in Eq. (14), we introduce now the assumption that the dependence of the stopping power  $S = dE/dx$  on ion energy  $E$  can be represented by a simple power law. In terms of the reduced energy  $\beta$ , and penetration distance  $\tau$ :

$$S(\beta) \equiv \frac{d\beta}{d\tau} = -\lambda \beta^n . \quad (18)$$

This assumption is particularly suitable for slow ions in solids. In particular, existing theories predict a proportionality of  $S$  with ion velocity ( $n = \frac{1}{2}$ ) [14-17] in fair agreement with experiments in the low-energy range [18-20]. Another possible choice could be to consider effective  $n$  values that approximate in a phenomenological way the dependence of the stopping power on ion energy, within a restricted energy range. With this approach the following derivation can be applied to intermediate and higher energies as well.

We now calculate the value of  $\Sigma$  in Eq. (14) as follows:

$$\Sigma = \int_0^\tau d\tau' \Delta(z') = \int_{\beta_0}^{\beta_1} \frac{d\beta}{(d\beta/d\tau')} \Delta\left(\frac{k}{\beta}\right) , \quad (19)$$

and using Eq. (18) we obtain

$$\Sigma = \frac{k^{1-n}}{\lambda} [G(z_1) - G(z_0)] , \quad (20)$$

where

$$G(z) = \int_0^z \frac{dz'}{z'^{2-n}} \Delta(z') . \quad (21)$$

Here  $\beta_0$  and  $\beta_1$  are defined as in Eq. (17), in terms of the mean energies  $E_0$  and  $E_1$  of the ions before and after traversing the foil, while  $z_0 = k/\beta_0$  and  $z_1 = k/\beta_1$  are the corresponding  $z$  values.

On the other hand, integrating the energy loss from

Eq. (18) we get

$$\frac{1}{\lambda} = \frac{\tau(1-n)}{\beta_0^{1-n} - \beta_1^{1-n}}, \quad (22)$$

and using this in Eq. (20) we finally obtain

$$\Sigma \equiv \tau \Delta(z_0, z_1) = \tau(1-n) z_0^{1-n} \frac{G(z_1) - G(z_0)}{1 - \mu^{1-n}}, \quad (23)$$

where the parameter  $\mu = \beta_1/\beta_0 = E_1/E_0$  is the ratio between the emerging and the incident ion energies ( $\mu < 1$ ), and hence  $(1-\mu)$  is the energy-loss fraction.

In the limit,  $\mu \rightarrow 1$ , from Eqs. (21) and (23) we get  $\Delta(z_0, z_1) \rightarrow \Delta(z)$  (with  $z = z_0 = z_1$ ), so that we retrieve the well-known multiple-scattering formulation, Eqs. (8)–(10), as derived by previous authors [10,11].

#### IV. CALCULATIONS

The following calculations have been made using the approximation formulas obtained by Kang, Kawatoh, and Shimizu [21], to the scattering function  $f(t)$ , for the so-called universal potential proposed by Ziegler, Bier-sack, and Littmark [22].

We will discuss first the results obtained without considering the effects of finite-energy losses.

In Fig. 1 we compare the values of the scattering function  $f(t^{1/2})$  in Eq. (1), for the universal potential (UP), the Thomas-Fermi (TF), and the Lenz-Jensen (LJ) potentials. As usual, the major discrepancies arise for small arguments; here the UP can be expected to provide a more adequate description [21,22].

We show in Fig. 2 the corresponding multiple-scattering function at zero angle,  $f_1(\tau, 0)$ , in Eqs. (8) and (9), for each potential. The results from the UP fall between those from the TF and LJ potentials, as expected from the behavior of the scattering functions in Fig. 1.

In Figs. 3(a) and 3(b) we show the angular distributions  $f_1(\tau, \alpha)$ , for two values of reduced thickness: (a)  $\tau = 0.1$  and (b)  $\tau = 1$ . As in the previous figures, the differences between the UP, TF, and LJ potential become negligible

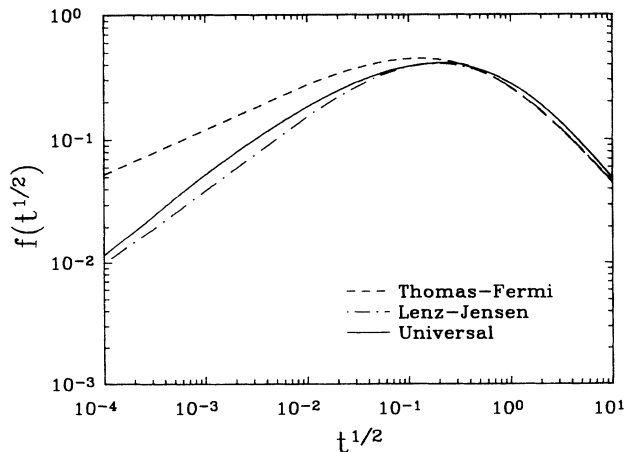


FIG. 1. Scattering function  $f(t^{1/2})$  in Eq. (1), calculated using the Thomas-Fermi, Lenz-Jensen, and the universal potentials.

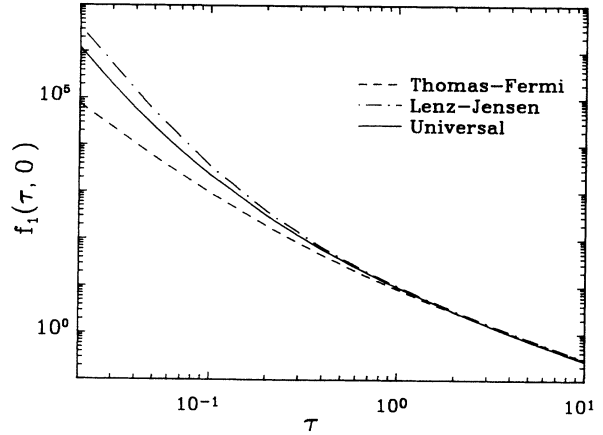


FIG. 2. Zero-angle multiple-scattering function  $f_1(\tau, 0)$ , as calculated from Eqs. (9) and (10), using the values for the scattering function  $f(t^{1/2})$  for the three model potentials illustrated in Fig. 1.

for larger values of  $\tau$  ( $\tau > 1$ ).

Finally, the half-widths, at half maxima  $\bar{\alpha}_{1/2}$  of the multiple-scattering distributions are shown in Fig. 4, for the three cases of interest.

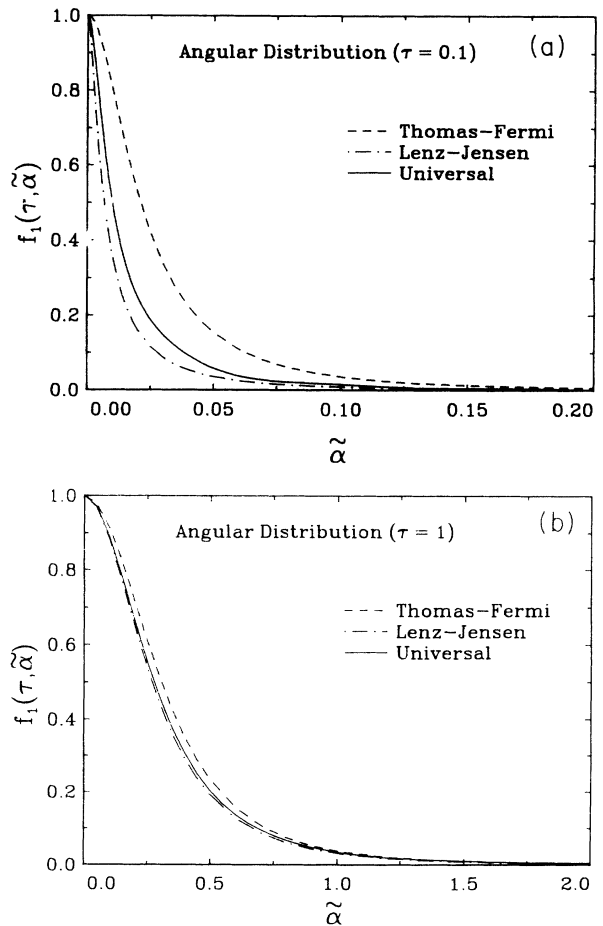


FIG. 3. Angular distribution function  $f_1(\tau, \bar{\alpha})$ , Eq. (9), for the three model potentials (Thomas-Fermi, Lenz-Jensen, and universal potential), as a function of reduced angle  $\bar{\alpha}$  and for reduced thicknesses  $\tau = 0.1$  (a) and  $\tau = 1$  (b).

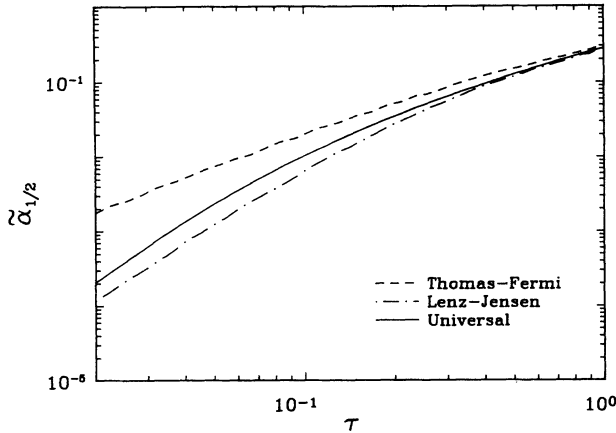


FIG. 4. Reduced half-width at half maxima  $\bar{\alpha}_{1/2}$  of the multiple-scattering distributions vs reduced thickness  $\tau$ , evaluated for the three model potentials (Thomas-Fermi, Lenz-Jensen, and universal potential).

Let us consider now the effects of finite-energy losses in the foil. From the derivation in the preceding section, and using the angle  $\varphi$  to denote the total multiple-scattering angle (previously called  $\alpha$ ) when energy loss is included, we can write

$$F(x, \varphi) d\Omega = \bar{\varphi} d\bar{\varphi} \int_0^\infty dz z J_0(z\bar{\varphi}) e^{-\tau\Delta(z, z/\mu)} \\ = \bar{\varphi} d\bar{\varphi} g_1(\tau, \bar{\varphi}, \mu), \quad (24)$$

where we have defined a new multiple-scattering function  $g_1(\tau, \bar{\varphi}, \mu)$ , which depends also on the energy ratio  $\mu = E_1/E_0$ . In Eq. (24) we have set

$$z \equiv z_0 = k/\beta_0, \quad (25a)$$

$$z_1 = k/\beta_1 = z/\mu, \quad (25b)$$

$$\bar{\varphi} = \beta_0 \varphi. \quad (25c)$$

We will consider in the following the case of a velocity-proportional stopping power [i.e.,  $n = \frac{1}{2}$  in Eqs. (18)–(23)], a case that is of general interest for the multiple scattering of slow ions. Then, the  $\Delta$  function in Eq. (24), for  $n = \frac{1}{2}$  becomes

$$\Delta(z, z/\mu) = \frac{1}{2} z^{1/2} \frac{G(z/\mu) - G(z)}{1 - \mu^{1/2}}, \quad (26)$$

with

$$G(z) = \int_0^z \frac{dz'}{z'^{3/2}} \Delta(z'), \quad (27)$$

where  $\mu = \beta_1/\beta_0$  and  $\Delta(z')$  is given by Eq. (15).

The function  $G(z)$ , calculated from the universal potential, is plotted in Fig. 5. The function  $\Delta(z, z/\mu)$ , with  $\mu = 0.5, 0.8$ , and  $1.0$ , is shown in Fig. 6. The curve for  $\mu = 1$  is identical to the function  $\Delta(z)$  of Eq. (15).

The effect of finite-energy loss on the angular-distribution function,  $g_1(\tau, \bar{\varphi}, \mu)$ , from Eq. (24), is illustrated in Fig. 7, for the case  $\tau = 0.5$ . Energy losses of 20% ( $\mu = 0.8$ ) and 50% ( $\mu = 0.5$ ) are shown in the figure,

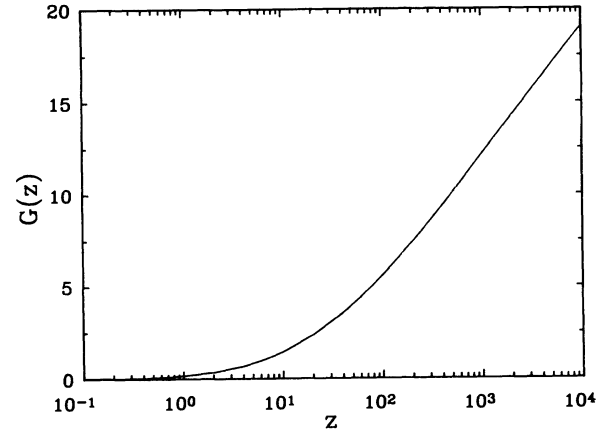


FIG. 5. Function  $G(z)$ , Eq. (27), for the calculation of multiple-scattering distributions with finite-energy losses in the medium. The present calculation corresponds to the case of a velocity-proportional stopping power ( $n = \frac{1}{2}$ ).

as well the distribution for  $\mu = 1$  (solid line), i.e., ignoring the energy loss in the medium. The enhancement of the distributions produced by the decrease of the ion energy in the target is illustrated in the inset of Fig. 7, which shows the normalized distributions.

From these distributions we can determine the half-widths (at half maxima) of the angular distributions. We will denote by  $\sigma_{1/2}$  and by  $\varphi_{1/2}$ , respectively, the half-widths of the distributions calculated according to the earlier (constant energy) formulas, Eqs. (8)–(10), and using the present variable-energy approach, Eqs. (24)–(27). The results of various calculations are compared in Fig. 8.

It has been proposed previously that one way to simulate the energy-loss effect on the multiple-scattering distributions would be to calculate the distributions from the standard theory (i.e., neglecting energy loss) but using

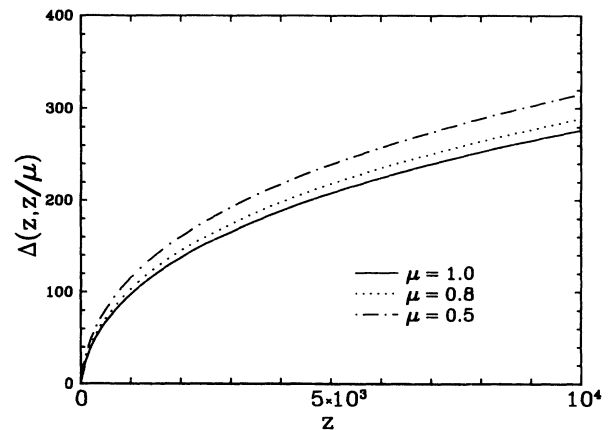


FIG. 6. Function  $\Delta(z, z/\mu)$ , Eq. (26), for the calculation of multiple-scattering distributions with finite-energy losses in the medium. The curves for  $\mu = 0.8$  and  $0.5$  correspond to 20% and 50% of energy loss in the target, while the curve for  $\mu = 1$  shows the results neglecting energy loss. The calculations correspond to the case of velocity-proportional stopping power ( $n = \frac{1}{2}$ ).

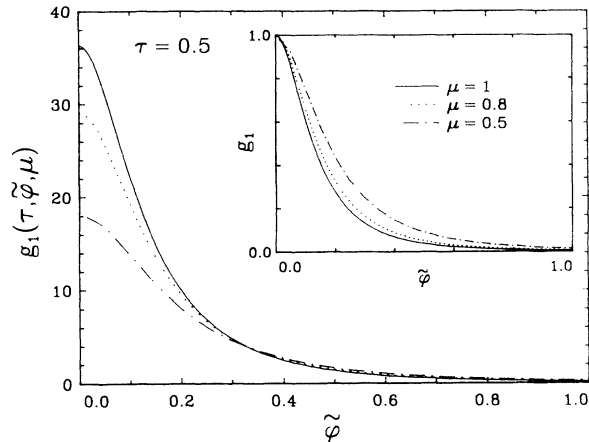


FIG. 7. Angular distribution function  $g_1(\tau, \bar{\varphi}, \mu)$ , Eq. (24), vs reduced scattering angle  $\bar{\varphi}$ , for  $\tau=0.5$  and for the three values of the energy-loss parameter  $\mu$  shown in Fig. 6. The inset shows the same distributions after normalization. The solid line ( $\mu=1$ ) corresponds to the case of negligible energy losses.

some average value for the energy of the ions during their transit through the target [5,7,8,13]. One can test this approach using the present description of the energy-loss effects.

In the range of low energies, using Eq. (18) with  $n = \frac{1}{2}$  for the stopping power, it can be shown that a convenient definition of the mean energy in the medium is the following [18,20]:

$$\beta_{m1} = \frac{1}{4}\beta_0(1 + \mu^{1/2})^2, \quad (28)$$

which corresponds to a straight average of the ion velocities before and after the interaction with the medium [ $\beta_0$  and  $\beta_1 = \mu\beta_0$  are the initial and final energies in the units of Eq. (7)].

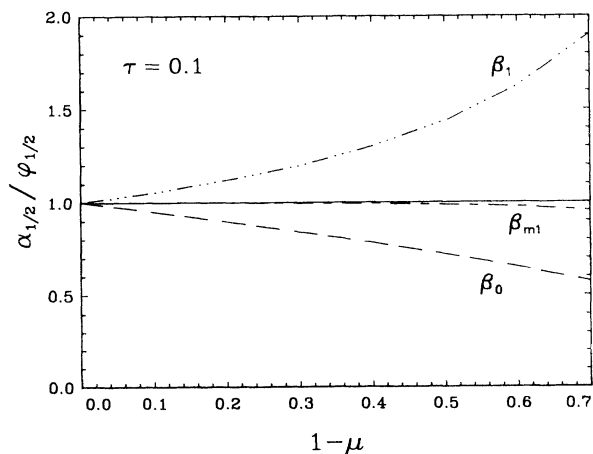


FIG. 8. Ratio of half-width at half maxima calculated without ( $\alpha_{1/2}$ ) and with ( $\varphi_{1/2}$ ) inclusion of the energy-loss effect, for  $\tau=0.1$  and as a function of the energy-loss parameter ( $1-\mu$ ). The curves for different  $\beta$  values correspond to approximations where the energy of the beam is assumed constant, equal to the initial ( $\beta_0$ ), final ( $\beta_1$ ), or to the average [ $\beta_{m1}$ , Eq. (28)] beam energy.

In Fig. 8 we show the ratios  $\alpha_{1/2}/\varphi_{1/2}$ , for values of the energy-loss parameter ( $1-\mu$ ) ranging from 0 to 0.7. The values of  $\alpha_{1/2}$  have been calculated neglecting the energy loss and for three mean energy values:  $\beta=\beta_0$  (incident beam energy),  $\beta=\beta_1$  (emerging beam energy), and  $\beta=\beta_{m1}$  [average of Eq. (28)], whereas the values of  $\varphi_{1/2}$  were computed with full account of the energy-loss effect. The curves start from  $\alpha_{1/2}/\varphi_{1/2} \cong 1$  at small energy losses ( $\mu \rightarrow 1$ ) and deviate for increasing  $1-\mu$ , to values below or above 1 depending on the  $\beta$  value. If the calculation is performed using the initial beam energy  $\beta_0$ , the angular distribution becomes too narrow (by more than 40% at the largest energy loss in the figure), while the opposite behavior is observed if the final beam energy  $\beta_1$  is considered (up to 90% larger than the exact result). The results using the mean energy  $\beta_{m1}$  of Eq. (28) compare surprisingly well, on a wide range of energy losses, to the integrations that incorporate the gradual beam-energy variation.

We finally note that other average values of the beam energy have been proposed [18,23], such as, in particular, the following:

$$\beta_{m2} = \frac{1}{3}\beta_0(1 + \mu + \mu^{1/2}), \quad (29a)$$

$$\beta_{m3} = \frac{1}{2}\beta_0(1 + \mu), \quad (29b)$$

$$\beta_{m4} = \frac{3}{5}\beta_0(1 - \mu^{5/2})/(1 - \mu^{3/2}). \quad (29c)$$

To test also these values in the low-energy range we performed similar calculations. We show in Fig. 9 the ratios  $\alpha_{1/2}/\varphi_{1/2}$ ; the  $\alpha_{1/2}$  values were calculated without energy loss, and for each of the  $\beta_m$  values in Eqs. (28) and (29). From this comparison we find that the average energy defined in Eq. (28) gives the best representation of the energy-loss effect of the angular half-widths for the case of slow ions. The agreement is better than 5% for  $1-\mu=0.7$  (i.e., 70% of energy loss).

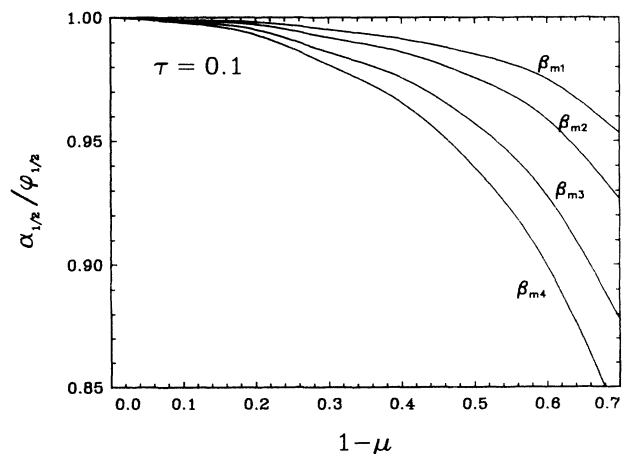


FIG. 9. Ratio of half-width at half maxima calculated without ( $\alpha_{1/2}$ ) and with ( $\varphi_{1/2}$ ) inclusion of the energy-loss effect, for  $\tau=0.1$  and as a function of the energy-loss parameter ( $1-\mu$ ). The curves for different  $\beta$  values illustrate various approximate descriptions of the energy-loss effect assuming constant (mean) energy values according to Eqs. (28) and (29).

## V. SUMMARY AND CONCLUSIONS

We have considered the incorporation of energy-loss effects in the multiple-scattering formulation. As described in Sec. III, these effects can be taken into account in a way that maintains the general scaling properties and the reduced variables from the standard multiple-scattering theory.

The new expression for the angular distribution  $g_1(\tau, \bar{\varphi}, \mu)$ , Eq. (24), contains, in addition to the reduced thickness and angle variables, a parameter  $\mu$  that represents the energy-loss fraction ( $1 - \mu$ ) of the ion beam after its passage through the target. The effect of the continuous energy variation is parametrized in the new scattering function  $\Delta(z, z/\mu)$  in Eq. (23). The present calculations show the increased spreads of the angular distributions due to the energy-loss effect.

Special consideration has been given to the case of slow ions in solids, in the range where the stopping power can be approximated by a simple velocity-proportional dependence. Such a dependence is predicted by various theoretical models [14–17] for ion velocities in the range  $v < v_0 Z_1^{2/3}$ .

The half-widths at half maxima of the distributions are compared with those calculated using the standard multiple-scattering theory. For the cases illustrated here,

we find that a simple account of the energy-loss effect on the angular distribution can be made by inserting in the earlier formulations [10,11] a mean ion energy inside the target which corresponds to the linear average of the incident and emerging ion velocities, as in Eq. (28).

We should note, however, that this particular value of the average energy is based on the low-velocity stopping-power approximation. Therefore, it should be expected that in other energy ranges somewhat different expressions for a “best” mean energy would apply [13]. A quantitative determination of the best average-energy expressions for various ranges of ion energies is a problem of practical interest, since it will allow us to estimate the energy-loss effect on the multiple-scattering distributions using the standard (fixed-energy) theory. A more extensive study of this problem can be made from the present formulation, but it lies beyond the scope of this work.

## ACKNOWLEDGMENTS

Useful comments by G. H. Lantschner and A. Gras-Martí are gratefully acknowledged. This work has been supported in part by Consejo Nacional de Investigaciones Científicas y Técnicas (CONICET, Argentina), through a research grant (PID 3-053100/88) and research support for J. E. Valdés.

- 
- [1] S. Goudsmit and J. L. Saunderson, *Phys. Rev.* **57**, 24 (1940); **58**, 36 (1940).
  - [2] G. Molière, *Z. Naturforsch.* **3a**, 78 (1948).
  - [3] H. S. Snyder and W. T. Scott, *Phys. Rev.* **76**, 220 (1949).
  - [4] W. T. Scott, *Rev. Mod. Phys.* **35**, 231 (1963).
  - [5] G. Högberg, H. Nordén, and H. C. Berry, *Nucl. Instrum. Methods* **90**, 283 (1970).
  - [6] H. H. Andersen and J. Bottiger, *Phys. Rev. B* **4**, 2105 (1971).
  - [7] H. H. Andersen, J. Bottiger, H. Knudsen, P. Moller Petersen, and T. Wohlenberg, *Phys. Rev. A* **10**, 1568 (1974).
  - [8] G. Sidenius and N. Andersen, *Nucl. Instrum. Methods* **128**, 271 (1975); **131**, 387 (1975).
  - [9] P. Sigmund, in *Interaction of Particles with Solids and Surfaces*, edited by A. Gras-Martí, H. M. Urbassek, N. R. Arista, and F. Flores (Plenum, New York, 1991).
  - [10] L. Meyer, *Phys. Status Solidi B* **44**, 253 (1971).
  - [11] P. Sigmund and K. B. Winterbon, *Nucl. Instrum. Methods* **119**, 541 (1974).
  - [12] D. Schmaus and A. L'Hoir, *Nucl. Instrum. Methods* **194**, 75 (1982).
  - [13] D. Schmaus and A. L'Hoir, *Nucl. Instrum. Methods B* **4**, 317 (1984).
  - [14] J. Lindhard, M. Scharff, and E. M. Schiott, *K. Dan. Vidensk. Selsk., Mat. Fys. Medd.* **33**, No. 14 (1963).
  - [15] J. Lindhard and A. Winther, *K. Dan. Vidensk. Selsk., Mat. Fys. Medd.* **34**, No. 4 (1964).
  - [16] O. B. Firsov, *Zh. Eksp. Teor. Fiz.* **36**, 1517 (1959) [*Sov. Phys. JETP* **9**, 1076 (1959)].
  - [17] P. M. Echenique, R. M. Nieminen, and R. H. Ritchie, *Solid State Commun.* **37**, 779 (1981); P. M. Echenique, R. M. Nieminen, J. C. Ashley, and R. H. Ritchie, *Phys. Rev. A* **33**, 897 (1986).
  - [18] R. Blume, W. Eckstein, and H. Verbeek, *Nucl. Instrum. Methods* **168**, 57 (1980).
  - [19] *Interaction of Particles with Solids and Surfaces*, edited by A. Gras-Martí, H. M. Urbassek, N. R. Arista, and F. Flores (Plenum, New York, 1991).
  - [20] J. E. Valdés, G. Martínez-Tamayo, G. H. Lantschner, J. C. Eckardt, and N. R. Arista, *Nucl. Instrum. Methods B* **75**, 313 (1993).
  - [21] H. J. Kang, E. Kawatoh, and R. Shimizu, *Jpn. J. Appl. Phys.* **23**, L262 (1984).
  - [22] J. F. Ziegler, J. Biersack, and U. Littmark, *The Stopping and Ranges of Ions in Matter* (Pergamon, New York, 1985), Vol. 1.
  - [23] S. H. Overbury, P. F. Dittner, S. Datz, and R. S. Thoe, *Rad. Effect* **41**, 219 (1979).